

RSC Advances



This is an *Accepted Manuscript*, which has been through the Royal Society of Chemistry peer review process and has been accepted for publication.

Accepted Manuscripts are published online shortly after acceptance, before technical editing, formatting and proof reading. Using this free service, authors can make their results available to the community, in citable form, before we publish the edited article. This *Accepted Manuscript* will be replaced by the edited, formatted and paginated article as soon as this is available.

You can find more information about *Accepted Manuscripts* in the [Information for Authors](#).

Please note that technical editing may introduce minor changes to the text and/or graphics, which may alter content. The journal's standard [Terms & Conditions](#) and the [Ethical guidelines](#) still apply. In no event shall the Royal Society of Chemistry be held responsible for any errors or omissions in this *Accepted Manuscript* or any consequences arising from the use of any information it contains.

1 **Effective heterogeneous electro-Fenton of m-cresol with iron loaded**
2 **active carbon**

3 Loubna Bounab^{a,b,c}, Olalla Iglesias^b, Elisa González-Romero^c, Marta Pazos^b and M. Ángeles
4 Sanromán^{b*}

5 *a Département de Chimie, Faculté des Sciences, Université Abdelmalek Essaâdi, 93030*
6 *Tétouan, Morocco*

7 *b Departamento de Ingeniería Química, Universidad de Vigo-Campus Vigo, 36310*
8 *Vigo, Spain*

9 *c Departamento de Química Analítica y Alimentaria, Universidad de Vigo-Campus*
10 *Vigo, 36310 Vigo, Spain*

11 **Corresponding author. Tel: +34 986 812383; fax: +34 986 812380; E-mail address:*
12 *sanroman@uvigo.es (M. Angeles Sanroman)*

13 **ABSTRACT**

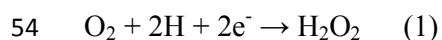
14 The degradation of m-cresol (MC) has been investigated by heterogeneous electro-
15 Fenton using iron loaded activated carbon (Fe-AC) as heterogeneous electro-Fenton
16 catalyst. Experimental results demonstrated that MC was effectively removed through
17 electro-Fenton. Calculated TOC removal and overall energy consumption showed that
18 the use of low iron concentration (28 mg/L) increases the efficiency of the process. The
19 reactions followed a pseudo-first order kinetic equation and kinetic coefficients confirm
20 that the MC reduction, when it is alone, is faster than in presence of a similar
21 compound, tert-butylhydroquinone (TBHQ) (from 0.0935 to 0.0692 min⁻¹); therefore
22 TBHQ exerts an antioxidative protection effect. In all cases, it is concluded that
23 heterogeneous electro-Fenton treatment with Fe-AC follows a process in two steps:
24 adsorption and oxidation; allowing removal rates higher than in the literature. In
25 addition, the reusability of this catalyst was showed operating in continuous mode.
26 Finally, LC-MS analysis allowed the development of a plausible degradation route.

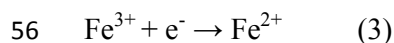
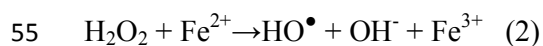
27
28 **Keywords:** m-cresol, tert-butylhydroquinone, continuous reactor, electro-Fenton, iron
29 loaded activated carbon.

30 Introduction

31 Cresols are an important sub-class of phenols reported by the United States
32 Environmental Protection Agency and the International Program on Chemical Safety as
33 priority pollutants due to their potential toxicity and their low biodegradation.¹⁻⁴ In
34 addition, cresols are extensively used in resin manufacturing, pharmaceuticals,
35 pesticides, tri-cresylic acid and surfactants, therefore it is released on the wastewaters
36 from those industries.¹ Thus, there is a great need for the development of a suitable
37 technology able to destroy efficiently these undesirable compounds. Several processes
38 have been developed on the treatment of phenol polluted wastewaters: biodegradation,^{5,}
39 ⁶ conventional physico-chemical methods such as adsorption,^{7, 8} and conventional
40 advanced oxidation processes (AOPs) such as photodegradation,^{9, 10} Fenton oxidation^{1,}
41 ¹¹ and their combinations.¹² However, some of these techniques require a low pollutant
42 concentration for an efficient pollutant removal or require the transportation, storage
43 and handling of hazardous reactants.^{5, 13}

44 Nowadays, electrochemical advanced oxidation processes (EAOPs) provide an
45 alternative that do not require the addition of reagent due to its generation from redox
46 reactions.¹⁴ Electro-Fenton has been reported as the most economic and promising
47 EAOP for the treatment of a wide variety of organic pollutants.¹⁵⁻¹⁹ The performance of
48 this process is based on the electrochemical *in situ* generation of H₂O₂ from the
49 continuous aeration on the cathode (eqn. (1)). Fe²⁺ present on the media catalyst the *in*
50 *situ* generation of highly oxidant hydroxyl radicals from H₂O₂ (eqn. (2)), furthermore
51 Fe²⁺ is continuously recycled by a direct cathodic reaction as shows eqn. (3). The
52 hydroxyl radicals produced are highly oxidative and non-selective molecules that
53 degrade the organic matter.²⁰⁻²²

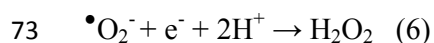
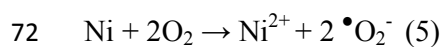




57 A crucial parameter for ensuring the appropriate performance of the electro-Fenton
58 process is the electrode material. Several articles reported the removal of m-cresol by
59 electro-Fenton process using GDE, Ti/SnO₂-Sb₂O₅-IrO₂ and PbO₂ electrodes.^{2, 23}
60 However, the last reports determined that boron-doped diamond electrodes (BDD) are
61 the most promising anode for EAOPs because they have significant characteristics, such
62 as corrosion stability, low adsorption properties and great oxidizing power to remove
63 organic pollutants.²⁴⁻²⁶ It can be ascribed to its high O₂-overpotential, which allows the
64 generation of high yields of the strong oxidant hydroxyl radical (BDD-HO[•]) adsorbed
65 on its surface from water oxidation (eqn. (4)).^{25, 27, 28}



67 Cathode material should optimize the generation of H₂O₂ among other reduction
68 reactions. Among the different materials that can be used as cathode, foam materials
69 have higher reaction surface, thus the use of nickel foam as cathode can improve the
70 production of hydroxyl radicals; furthermore the presence of nickel produces an
71 additional H₂O₂ generation from the superoxide radical (eqn. (5) (6)).²⁹



74 Industrial activities constantly produce wastewaters that need a treatment. Therefore, it
75 is necessary to validate an adequate technique to continuously remediate polluted
76 streams. In electro-Fenton process iron on solution gets away on the outflow. Therefore,
77 it is further necessary to improve the electro-Fenton technology in order to reduce this
78 problem and reduce the investment and operation costs. Several studies have focused on
79 the immobilization of iron on supports with physical characteristics that avoid its lost.^{15,}

80 ³⁰ Activated carbon (AC) is characterized by its great absorption capacity and it has
81 already been used as iron support with different environmental applications.³¹⁻³³ In order
82 to overcome the main drawback of the electro-Fenton process operating in continuous
83 mode in this study the use of iron loaded in AC (Fe-AC) is considered a workable
84 solution.

85 The aim of this work is to design an electro-Fenton continuous reactor with BDD as
86 anode and nickel foam as cathode to treat polluted effluents in a continuous mode at the
87 bench scale using Fe-AC as Fenton catalyst. To analyse the technique's capacity, m-
88 cresol and tert-butylhydroquinone were used as model pollutants.

89 **Experimental**

90 **Materials**

91 In this study, solutions of m-cresol (MC) (100 mg/L) and tert-butylhydroquinone
92 (TBHQ) were provided by Sigma-Aldrich (Barcelona, Spain) and used in order to
93 evaluate the electro-Fenton treatments. Their structure and properties are shown in
94 Table 1.

95 **Catalyst preparation and characterization**

96 Iron load on activated carbon (Fe-AC) was carried out by mixing a constant volume
97 (0.15 L) of iron aqueous solution at 1000 mg/L of Fe³⁺ (Fe₂SO₃; Sigma-Aldrich, Spain)
98 with 3 g of Activated Carbon (AC) (Granulated n°2 QP Panreac Spain) in 0.25 L
99 Erlenmeyer flasks. The flasks were agitated in an incubator (Thermo Forma 420) at 150
100 rpm and 20°C for 30 minutes. The phenantroline method 3500 D (Standard Methods- 18
101 Ed. 1992) was used to measure the iron that remained unabsorbed in the supernatant

102 liquid. Finally, the resulting Fe-AC composite was dried in an oven at 105°C and stored
103 at room temperature.

104 Fe-AC was characterized by Scanning Electron Microscopy (SEM) performed on a
105 JEOL JSM-6700F equipped with an Energy Dispersive Microanalysis (EDS) Oxford
106 Inca Energy 300 SEM using an accelerating voltage of 20 kV (Electron Microscopy
107 Service, C.A.C.T.I., University of Vigo).

108 **Electro-Fenton reactor set-up**

109 The heterogeneous electro-Fenton with Fe-AC was performed in a cylindrical glass
110 reactor with a working volume of 0.15 L. The electric field (5 V) was applied by a 1.6
111 mm thick nickel foam cathode (Goodfellow Cambridge Ltd, United Kingdom) and a
112 BDD anode (DIACHEM®, Germany) connected to a direct current power supply (HP
113 model 3662, Agilent Technologies Spain, S.L.). The electrodes (surface 15 cm²) were
114 placed opposite to each other at 1 cm above the bottom of the cell and with an electrode
115 gap of 6 cm. Current intensity was monitored with a multimeter (Fluke 175). H₂O₂ was
116 continuously electrogenerated *via* oxygen reduction on the cathode, by bubbling 1
117 L/min of compressed air. Reaction mixture contains 150 ml of solution Na₂SO₄ (0.01
118 M) as electrolyte, 100 mg/L of phenolic compound and 3 g of Fe-AC at different iron
119 concentrations (46 mg/L and 28 mg/L). The pH was adjusted to 2 by the addition of
120 sulphuric acid (Sigma Aldrich, Spain). The medium was maintained in suspension by
121 magnetic stirring avoiding concentration gradients in the cell.

122 **Sample preparation and preservation**

123 For all experiments, 1 mL samples were taken periodically from the reactor,
124 centrifuged (Sigma 3K-18) for 10 minutes at 7000 rpm to remove solid and stored at
125 4°C until chemical analysis.

126 Analytical procedures

127 A survey of literature describes the analytical methods available for quantifying,
128 monitoring and detecting phenolic compounds.³⁴ In this work, HPLC, LC-MS and TOC
129 analysis were performed.

130 The concentrations of MC and TBHQ were quantified by means of HPLC (Agilent
131 1100) equipment with an XDF-C8 reverse-phase column (150 x 4.6 mm i.d., 5 μ m).
132 Prior to injection, the samples were filtered through a 0.45 μ m Teflon filter. The
133 injection volume was set at 10 μ L, and the gradient of eluent (acetonitrile/water with a
134 1.5 % of acetic acid) was pumped at a rate of 1 mL/min for 20 minutes. Detection was
135 performed with a diode array detector at 274 nm for MC and 292 nm for TBHQ, and the
136 column was maintained at room temperature.

137 In order to identify the transformation products obtained in the MC degradation several
138 samples were analyzed with an LC-MS (Agilent 1100) equipment with a LC column
139 ZORBAX. Filtration through a 0.45 μ m Teflon filter was done before the injection. In
140 this case the isocratic eluent was 90 (water):10 (acetonitrile) that was pumped at a rate
141 of 0.5 mL/min for 40 minutes. Detection was carried out with a diode array detector at
142 218 nm and the column temperature was maintained at 23°C. The coupled mass
143 spectrometer employed was a Hewlett-Packard 5989B with a detection range from 10 to
144 2000 Da.

145 Total Organic Carbon (TOC) in aqueous solutions was determined by using a Lange
146 cuvette test (LCK 380) in a Hanch Lange DR 2800, according to stand method DIN
147 38409-H3. The sample was introduced in the Lange cuvette. Under the conditions of the
148 test, the carbon forms carbon dioxide, which diffuses through a membrane into an

149 indicator solution. The change of color of the indicator solution is evaluated
150 photometrically.

151 H₂O₂ concentration was determined by the titanium oxalate method.³⁵ The method is
152 based on the generation of a yellow-orange titanium (IV) peroxide complex with a
153 maximum absorbance at 400 nm. Thus, 2 mL of sample are mixed with 0.25 mL of
154 sulphuric acid (0.5 mmol/L), 0.2 mL of potassium titanium oxide oxalate dehydrate
155 (0.14 mol/L) and 0.05 mL of distilled water for a final volume of 2.5 mL, after 5
156 minutes the absorbance was measured spectrophotometrically. All reagents were
157 provided by Sigma-Aldrich (Barcelona, Spain).

158 **Kinetic studies**

159 Kinetic studies were done in order to model the behavior of the heterogeneous EF-Fe-
160 AC. The concentration profiles of selected degradation compounds were fitted by a
161 suitable kinetic equation and the rate constants were calculated by using SigmaPlot 4.00
162 (1997) software. The SigmaPlot curve fitter uses an iterative procedure, based on the
163 Marquardt-Levenberg algorithm, which seeks the values of the parameters that
164 minimize the sum of the squared differences between the observed and predicted values
165 of the dependent variable.

166 **Measurement of process efficiency**

167 In addition to analyzing compounds concentration and therefore their removal during
168 the experiments, other specific energetic parameter is useful such as energy
169 consumption per amount of TOC destroyed (eqn. (7)) were evaluated.

$$170 \quad \text{Energy consumption (kWh / kg}_{\text{TOC}}) = \frac{I \cdot V \cdot t}{(\Delta m_{\text{TOC}}) V_s} \quad (7)$$

171 where I is the average applied current (A), V is the cell voltage (V), t is the treatment
172 time (h), V_s is the solution volume (L) and Δm_{TOC} is the decay in TOC concentration
173 (g/L)

174 **Continuous EF-FeAC process set-up**

175 An electrochemical cell with the same characteristics than the one used for the batch
176 experiments was selected (Fig. 1). The electro-Fenton reactor had a working volume of
177 0.15 L with 3 g of FeAC at an iron concentration of 28 mg/L and pH 2. H_2O_2 was
178 produced electrochemically by bubbling compressed air near the cathode at
179 approximately 1 L/min. The polluted solution was homogenized by a magnetic stirrer.
180 A dual-headed peristaltic pump was used to maintain a continuous flow of MC solution
181 through the reactor. Samples from the outlet flow were frequently taken to measure pH
182 and analyze MC concentration. The reactor operated in continuous mode at residence
183 times of 45 and 60 minutes. In all cases, each steady-state was maintained for at least
184 three times the residence time.

185 **Results and Discussion**

186 **Heterogeneous electro-Fenton treatment of MC**

187 Initially, the preparation of Fe-AC was carried out by adsorption technique. Due to
188 precipitation of the Fe^{3+} as iron hydroxide, it is not possible to carry out adsorption
189 experiments with iron at $\text{pH} > 4.0$. For this reason, in these experiments, the natural pH
190 of the iron solution was used. The kinetic of iron adsorption can provide valuable
191 insights about the reaction pathways and mechanisms of the reaction. The kinetic and
192 thermodynamic behaviour of the adsorption reaction fitted very well to a pseudo-

193 second-order model and the adsorption is endothermic in nature and mainly physical.³⁶⁻
194 ³⁸

195 In order to verify the adsorption of iron onto AC a Scanning Electron Microscopy and
196 Energy Dispersive Spectrometry (SEM/EDS) was performed. EDS is an analytical
197 technique used for the elemental analysis or chemical characterization of a sample. As
198 can be seen in the SEM images (Fig. 2), AC has high porosity and consequently a good
199 adsorption capacity. In addition, EDS spectral analysis confirms the increasing of iron
200 onto the Fe-AC after the adsorption process. The elementary composition of the AC
201 indicates that there is not iron with a carbon content of 89.19%, however this value
202 change after the adsorption and the composition of Fe-AC is 84.61% of carbon and the
203 iron concentration increased up to 2.53%. These results reflected that iron specie
204 remained homogeneously onto the AC structure (Fig 2B).

205 The electro-Fenton process with Fe-AC was conducted in batch mode with two initial
206 iron concentrations 46 mg/L and 28 mg/L on Fe-AC. Fig. 3 shows the profile of MC
207 reduction along the treatment time. As can be observed, the heterogeneous electro-
208 Fenton with a lower iron concentration on Fe-AC improves the rate of MC reduction.
209 Thus, it was determined that the best iron concentration is 28 mg/L in order to carry out
210 the electro-Fenton reactions with Fe-AC for the treatment of MC. This result is in
211 agreement with several other studies such as the cresol degradation by Fenton process
212 and phenol degradation by electro-Fenton and sono-electro-Fenton processes.^{1, 39} In
213 these studies, it was reported that a further increase in Fe²⁺ ion concentration did not
214 correspondingly increase its reactivity, probably due to direct reaction of hydroxyl
215 radical with metal ions. In addition, our results are in concordance with other previous
216 results in which it is postulated that AC is able to decompose hydrogen peroxide and,

217 therefore, to generate hydroxyl radical. For this reason, it is not necessary the presence
218 of a high iron concentration into AC.⁴⁰

219 In this experiments the H₂O₂ was generated and transformed in Fenton's reactions and
220 the H₂O₂ concentration was around 0.3-0.4 mmol/L. This fact is due to air and nickel
221 react to generate H₂O₂ as described in equation 5 and 6, this results are in accordance
222 with those obtained by Liu²⁹ who reported the improvement on the H₂O₂ generation and
223 consequently the hydroxyl radical generation. Moreover, the regeneration of Ni²⁺ due to
224 the electric field avoids the nickel ions leaching and the electrode keeps its structure and
225 composition along the treatment.

226 The MC concentration profiles allow the evaluation of the kinetic behavior of this
227 reaction. The obtained data were adjusted to several orders and the best fit was obtained
228 when a pseudo-first-order kinetic expression was used (eqn. (8)).

$$\frac{dC}{dt} = -kC \quad (8)$$

229 where *C* is concentration of MC (mg/L); *t* is reaction time (min) and *k* is kinetic
230 coefficient for the pseudo-first order reaction (min⁻¹).

231 This result is in accordance with the postulated by Lucas & Peres⁴¹ for the Fenton
232 treatment of olive mill wastewater and the electro-Fenton treatment of MC. They
233 concluded that the reaction kinetic behavior could be represented by a simple
234 irreversible reaction of pseudo-first-order kinetics with respect to MC concentration.
235 This behavior was also corroborated by Chu⁴².

236 The rate constants values and the statistical correlation parameters are shown in Fig. 4.
237 As expected from the degradation profiles, the highest kinetic parameter value was
238 $k=0.0935 \text{ min}^{-1}$ to lower iron concentration (28 mg/L). Chu⁴² surveyed the effect of iron

239 and initial MC concentration on the decay kinetics of electrochemical degradation of
240 MC using porous carbon-nanotube-containing cathode and Ti/SnO₂-Sb₂O₅-IrO₂ anode.
241 They observed that the kinetic parameter value (0.0239 min⁻¹) obtained with 33.6 mg/L
242 of iron was evidently lower than the value (0.0276 min⁻¹) obtained at an iron
243 concentration of 22.4 mg/L. Although the effect of iron was similar, the kinetic values
244 and the reaction rate were higher around 4-fold than reported in the literature³⁷.

245 This fact could be due to the use of this catalyst Fe-AC. It is known that AC has a high
246 adsorption capacity, which has been widely studied for the treatment of different
247 polluted wastewaters.^{31, 43, 44} Detailed explanation of the application of AC to phenolic
248 adsorption has been given by Busca.⁴⁵ As it is mentioned in previous papers the
249 heterogeneous electro-Fenton treatment is a process that takes place in two steps.^{15, 46}
250 Initially, the pollutant is adsorbed on the catalyst and after it is degraded by oxidation
251 reactions.

252 For testing this hypothesis, the adsorption on Fe-AC of MC and MC desorption after
253 electro-Fenton treatment was evaluated. As it can be seen in Fig. 5 a high adsorption
254 rate was detected, reaching a total MC reduction by adsorption after 120 minutes.
255 However, in the heterogeneous electro-Fenton process, near complete reduction is
256 achieved after 45 minutes (Fig. 3). Fe-AC proved to have a very high adsorption
257 capacity that did not reach the saturation after 3 cycles of 0.15 L of MC solution on 3g
258 of Fe-AC at an iron concentration of 28 mg/L.

259 Thus, these results indicate that the electro-Fenton of MC in heterogeneous electro-
260 Fenton with Fe-AC is a process that couples adsorption and degradation, for this reason
261 after 90 minutes of electro-Fenton treatment, the remaining MC adsorbed on the Fe-AC

262 is nearly the 1% of initial concentration. This results prove that adsorption on Fe-AC is
263 followed by a fast degradation on the Fe-AC surface.

264 The TOC measurements show a similar behaviour as the MC reduction, though they
265 need more treatment time to reach the complete mineralization. Thus, after 120 minutes
266 of treatment, TOC was reduced by 67.3% with 46 mg/L of iron and 83% with 28 mg/L
267 of iron and the energy consumption per TOC reduced was 29.7 and 15.1 kWh/kg_{TOC}
268 operating with initial iron concentrations of 46 mg/L and 28 mg/L, respectively. This
269 study has shown that the energy consumption from the system operating at the lower
270 iron concentration was about 2 folds of magnitude lower than those obtained at initial
271 iron concentrations of 46 mg/L.

272 These TOC values were greater to that found by Isarain-Chávez⁴⁷ for mineralization of
273 organic pollutants by combined electrocoagulation and photoelectro-Fenton processes
274 (70% in 180 minutes) and Liu⁴⁸ in the catalytic wet peroxide oxidation of MC; in which
275 the TOC removal reached 51.0% after 120 minutes of treatment. These results
276 demonstrate the efficiency of the heterogeneous electro-Fenton with Fe-AC, which
277 quantitatively reduces the organic load.

278 **Heterogeneous electro-Fenton treatment of TBHQ alone and in combination of** 279 **MC**

280 TBHQ is an antioxidant used on biodiesel to prevent its spoiling.⁴⁹ This molecule was
281 selected to evaluate its effect on the treatment of MC due to its similar structure and
282 composition. For this reason, the electro-Fenton process was carried out at the optimal
283 conditions (pH 2, 0.01 M of Na_2SO_4 and 28 mg/L of iron concentration) to degrade a
284 TBHQ solution and its combination with MC (Fig. 6).

285 Fig. 6 shows that the reduction of MC when TBHQ is present on the solution is lower
286 than alone. In all cases, TBHQ is reduced faster than MC. The reduction of TBHQ is so
287 fast that it is not modified in presence of MC. The kinetic study of the different
288 treatments shows a pseudo-first order and the values of their kinetic coefficient confirm
289 the aforementioned tendency, with a faster reduction of MC, when it is alone, than in
290 presence of TBHQ (from 0.0935 to 0.0692 min⁻¹) (Fig. 4). Therefore TBHQ seem to
291 have an antioxidative protection of MC reducing its decomposition.

292 In addition, the adsorption of TBHQ on Fe-AC was studied. It is detected a faster
293 adsorption and all TBHQ is removed from the solution after 30 minutes; however in the
294 electro-Fenton treatment the total reduction was achieved after 20 minutes.
295 Furthermore, after a heterogeneous electro-Fenton with Fe-AC of TBHQ there is not
296 TBHQ adsorbed on Fe-AC, which confirms the efficiency of the treatment. This fact
297 confirms again the hypothesis of a combined process with adsorption in catalyst
298 followed by the degradation action of hydroxyl radical.

299 To verify the efficiency in the organic pollutant degradation by heterogeneous electro-
300 Fenton with Fe-AC, the reduction in TOC was evaluated in all reaction media
301 employed. TOC was not significantly influenced by the presence of several compounds
302 in the reaction media. High TOC reduction 91.2% and 91.3% was detected after 120
303 minutes treatment of TBHQ alone and in combination of MC, respectively. This values
304 are higher that found in the literature. Izaomen⁵⁰ studied the degradation of o-cresol and
305 p-cresol by Fenton and photo-Fenton. They found that photo-Fenton process was more
306 efficient than Fenton in the mineralization and 90% of TOC removal was achieved in
307 150 minutes of UV.

308 **Continuous heterogeneous electro-Fenton treatment of MC**

309 In order to evaluate the activity and stability of the catalytic action of the Fe-AC and
310 minimize site requirements for the treatment of large amounts of wastewater, a
311 continuous mode for the electro-Fenton with Fe-AC of MC at different residence times
312 was tested. The process took place in a reactor of similar characteristics than the one
313 used for batch experiments and described in experimental and Fig. 1. Initially the
314 hydrodynamic behaviour of this reactor was studied through the residence time
315 distribution (RTD) curves. These tracer experiments were carried out at different flow
316 rates to confirm that the reactor used in this work closely matches ideal mixing
317 conditions. Thus, the reactor behaved as a continuous stirred-tank reactor (CSTR) and it
318 can be assumed that the concentration everywhere in the reactor is equal to the outlet
319 concentration and the fluid has a mean residence time equal to the reactor volume
320 divided by the volumetric flow rate through the tank.

321 To model this process it is necessary to include the kinetic behaviour determined in the
322 previous batch experiments. An expression that relates the reduction of MC and
323 residence times was obtained on the basis of the CSTR hydrodynamic behaviour and the
324 first order kinetic model. It is shown in eqn. (9).

$$325 \quad R = 100 \cdot \frac{k \cdot \tau}{1 + k \cdot \tau} \quad (9)$$

326 where R is the percentage of MC reduction, k is the previously obtained kinetic
327 coefficient for the first order reaction (min^{-1}) and τ is the residence time (min).

328 Fig. 7 shows the increase of reduction percentage with the residence time, attaining 72%
329 for a residence time of 45 minutes and 80% for a residence time of 1 hour. The value of
330 energy consumption per TOC reduced was found to be 8.2 kW h/kg_{TOC} and

331 corresponding to TOC removal efficiency of 83.4%, demonstrating adequate low energy
332 consumptions.

333 In addition, the theoretical reduction values were calculated using Eq. (9) for the two
334 employed residence times, and they are represented in Fig. 7 as the long dashed line.
335 The proposed model was able to satisfactorily describe the MC reduction data and to
336 serve our goal of properly characterizing the kinetics of the remediation process.

337 **Analysis of MC degradation compounds**

338 In order to identify the transformation products obtained in the MC degradation, several
339 samples were analyzed with LC-MS. The LC-MS study of MC solution treated in the
340 heterogeneous electro-Fenton with Fe-AC was carried out at initial time, after 3 hours
341 and after 24 hours.

342 At initial time several compounds with a phenolic group are found, while its intensity is
343 very low and increases with treatment time. MC is only found at initial time, after 3
344 hours of treatment there are intermediate products that were identified and after 24
345 hours just a few compounds are found and identified. Among the phenolic derivatives
346 found, 2-methylhydroquinone appears at initial degradation times and 2-methyl-p-
347 benzoquinone appears after 3 hours; however none of them appear after 24 hours of
348 treatment time. These compounds were detected by Flox,² Flox¹² and Chu⁴² as
349 intermediate products in different EAOPs of MC. The degradation pathway is
350 represented in Fig. 8. Similar reaction sequence for the electro-Fenton degradations of
351 MC in acid medium using a BDD anode was proposed by Flox.¹²

352 **Conclusion**

353 In the present work, the heterogeneous electro-Fenton process used Fe-AC as catalyst
354 for the degradation of MC. The performance of this technique is characterized by the
355 following:

- 356 - AC demonstrated its capacity to absorb iron and to perform as catalyst on the
357 heterogeneous electro-Fenton treatment.
- 358 - The evaluation of iron dosage showed that 28 mg/L contains the required
359 amount to the electro-Fenton reactions to take place, besides AC has been found
360 in literature as competitor on the hydroxyl radical production.
- 361 - The heterogeneous electro-Fenton treatment with Fe-AC has proved to be a
362 process where adsorption is followed by oxidation leading a decontaminated
363 wastewater and a pollutant free catalyst.
- 364 - The analysis of antioxidant TBHQ showed the capacity of this compound to
365 slow down the MC degradation.
- 366 - Kinetic studies demonstrated that the process follows a pseudo-first-order
367 kinetic equation which shows that 28 mg/L of iron behaves faster than 46 mg/L
368 and that the presence of TBHQ diminishes the kinetic constant.
- 369 - The study of energy consumption and TOC removal further confirmed the
370 efficiency of the developed process to the degradation of MC.
- 371 - Finally, the identification of a plausible degradation route eases the
372 understanding of process oxidation pathways.

373

374 **Acknowledgements**

375 This research has been financially supported by the Spanish Ministry of Economy and
376 Competitiveness, Xunta de Galicia and ERDF Funds (Projects CTM2011-26423, GRC

377 2013/003 and R2014/030). The authors are grateful to the Spanish Ministry of Economy
378 and Competitiveness for financial support of the researcher Marta Pazos under a Ramón
379 y Cajal program and Erasmus Mundus Green IT Program from EACEA-European
380 Union (REF: 2012-2625/001-001-EM-Action2-Partnerships-Staff mobility 2014) for
381 research stay of Loubna Bounab.

382

383

384

385 **Table and figure captions**

386 **Fig. 1.** Schematic diagram of electro-Fenton experimental set-up in continuous
387 processing: (1) Nickel foam acting as cathode, (2) BDD electrode acting as anode, (3)
388 powersupply, (4) air supply, (5) magnetic stirrer, (6) dual-headed peristaltic pump, (7)
389 inlet flow, (8) outlet flow.

390 **Fig. 2.** A. Scanning electron microscopy (SEM) image of Fe-AC and B. Fe mapping of
391 energy dispersive scanning spectroscopy (EDS) of Fe-AC.

392 **Fig. 3.** Profiles of MC reduction by heterogeneous electro-Fenton with Fe-AC at an iron
393 concentration of 46 mg/L (black squares) and 28 mg/L (black circles).

394 **Fig. 4.** Pseudo-first-order kinetic equation of heterogeneous electro-Fenton of MC
395 (black circles) working with 28 mg/l of iron, MC in presence of TBHQ (white circles)
396 working with 28 mg/l of iron and MC (black squares) working with 46 mg/l of iron.

397 **Fig. 5.** Batch adsorption profiles of MC on Fe-AC. Each batch contained 100 mg/L of
398 MC at pH 2 and 0.01 M of Na₂SO₄.

399 **Fig. 6.** Profiles of MC and TBHQ reduction by heterogeneous electro-Fenton with Fe-
400 AC at an iron concentration of 28 mg/L in different reaction media: MC alone (black
401 circles), MC in presence of TBHQ (white circles), TBHQ alone (black triangles) and
402 TBHQ in presence of MC (white triangles).

403 **Fig 7.** Continuous electro-Fenton with Fe-AC (28 mg Fe/L) treatment of MC at two
404 residence times (45 and 60 min); dotted lines correspond with the theoretic reduction
405 from the kinetic behaviour.

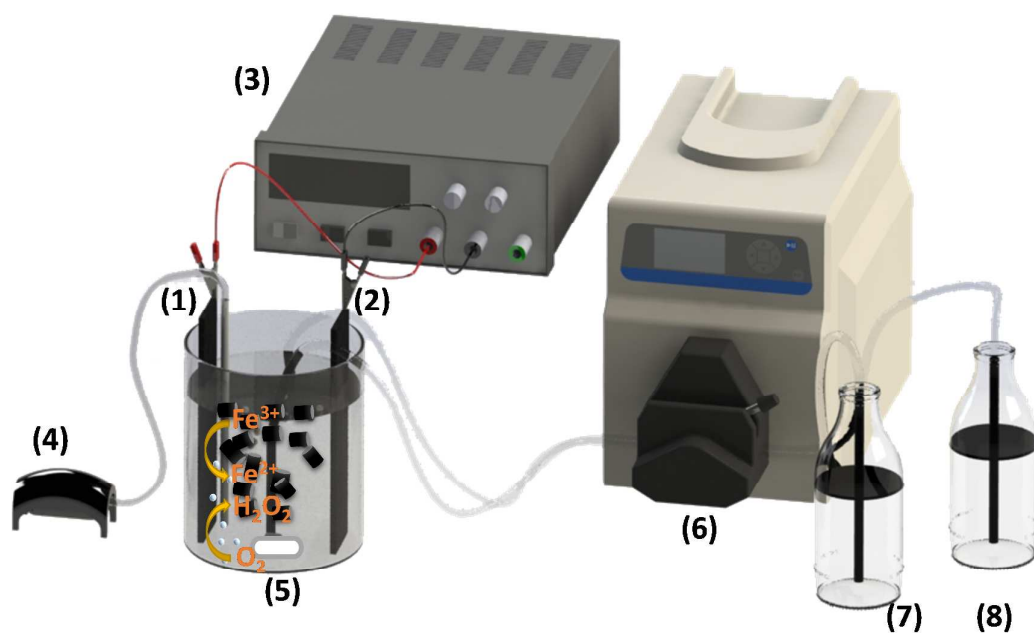
406 **Fig. 8.** Proposed reaction sequence on the degradation of m-cresol by the heterogeneous
407 electro-Fenton with Fe-AC.

408 **Table 1.** Chemical formula and structure, CAS number and concentration of studied
409 compounds.

410

411

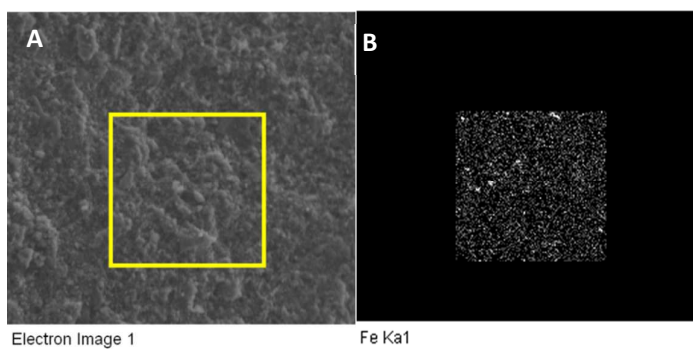
412



413

414 **Fig. 1.** Schematic diagram of electro-Fenton experimental set-up in continuous
415 processing. Nickel foam acting as cathode (1), BDD electrode acting as anode (2),
416 powersupply (3), air supply (4), magnetic stirrer (5), dual-headed peristaltic pump (6),
417 outlet flow (7), inlet flow (8).

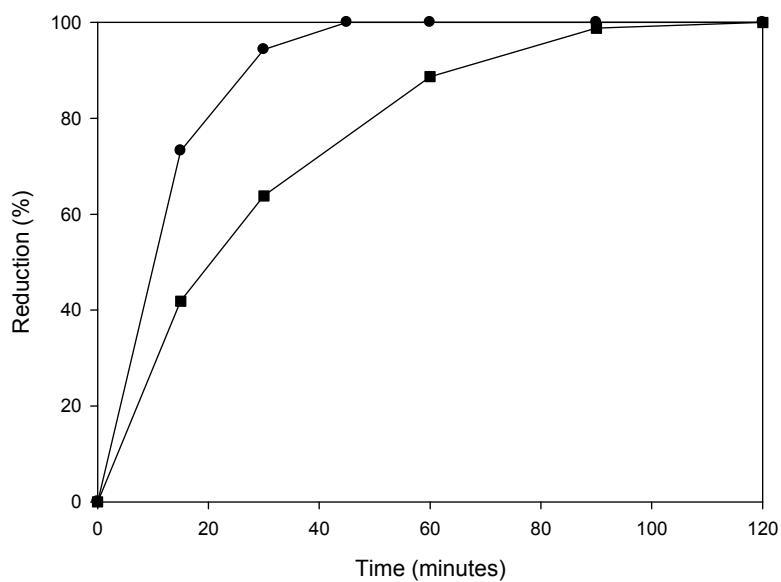
418



419

420 **Fig. 2.** A. Scanning electron microscopy (SEM) image of Fe-AC and B. Fe mapping of
421 energy dispersive scanning spectroscopy (EDS) of Fe-AC.

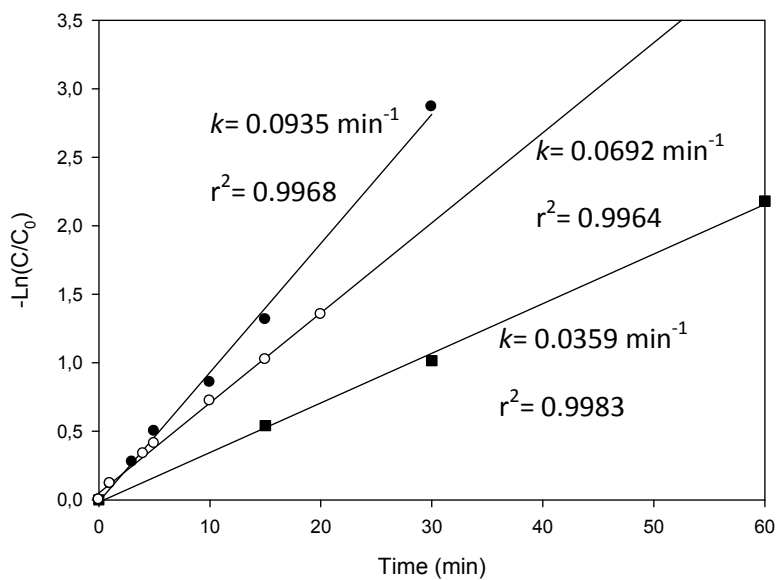
422



423

424 **Fig. 3.** Percentage of MC reduction with treatment time in the heterogeneous electro-
425 Fenton with Fe-AC at an iron concentration of 46 mg/L (black squares) and 28 mg/L
426 (black circles).

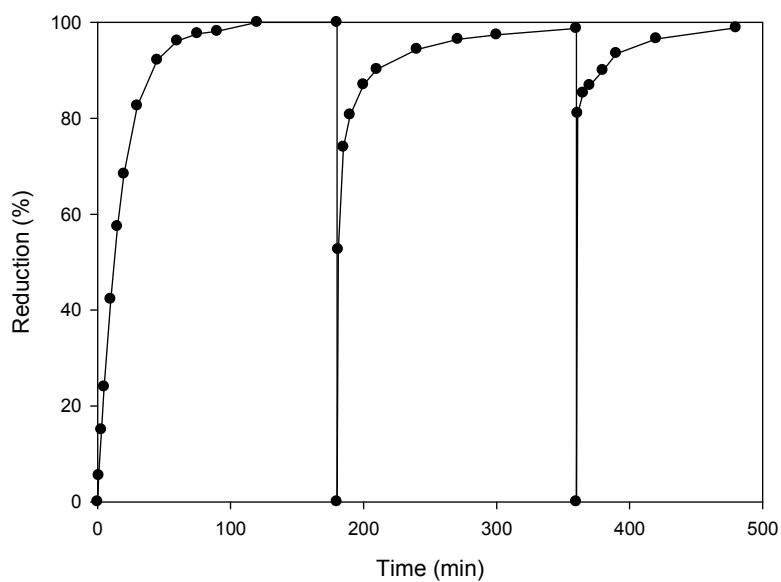
427



428

429 **Fig. 4.** Integrated pseudo-first-order kinetic equation and its constants extracted from
430 the slope, of heterogeneous electro-Fenton of MC (black circles) working with 28 mg/L
431 of iron, MC in presence of TBHQ (white circles) working with 28 mg/L of iron and MC
432 (black squares) working with 46 mg/L of iron.

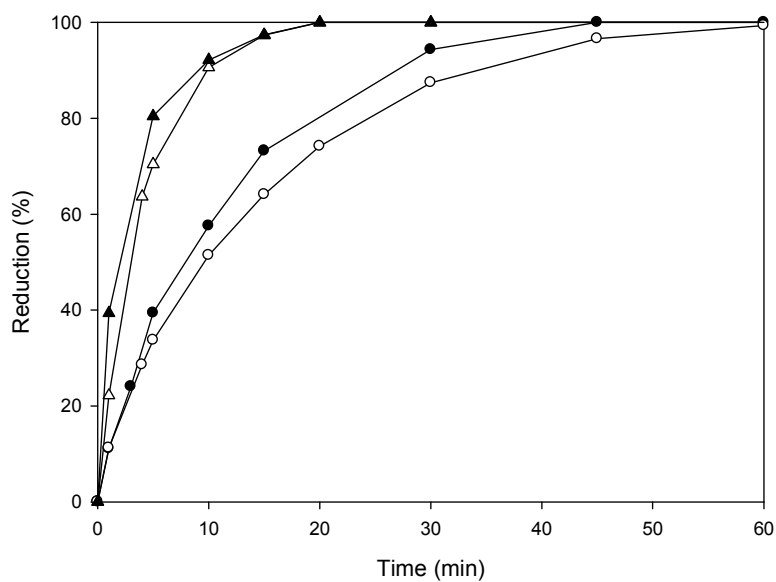
433



434

435 **Fig. 5.** Batch adsorption profiles of MC on Fe-AC. Each batch contained 100 mg/L of436 MC at pH 2 and 0.01 M of Na₂SO₄.

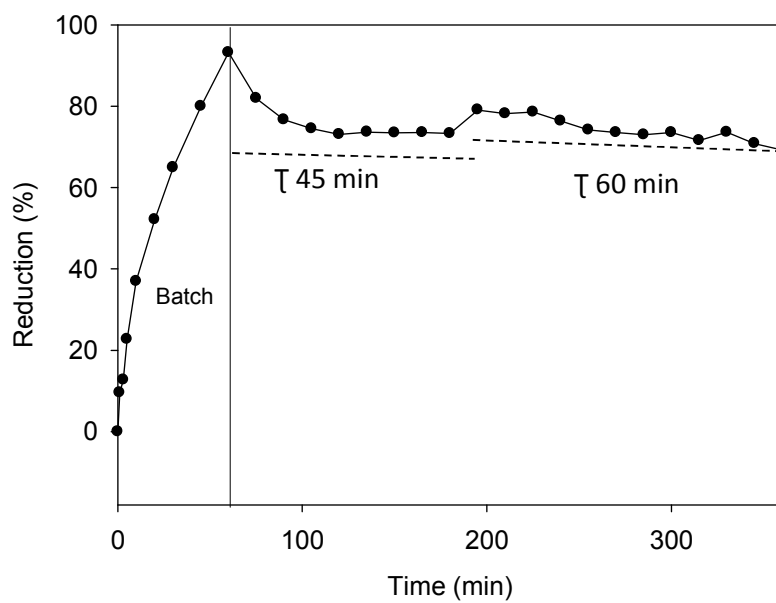
437



438

439 **Fig. 6.** Profiles of MC and TBHQ reduction by heterogeneous electro-Fenton with Fe-
440 AC at an iron concentration of 28 mg/L in different reaction media: MC alone (black
441 circles), MC in presence of TBHQ (white circles), TBHQ alone (black triangles) and
442 TBHQ in presence of MC (white triangles).

443



444

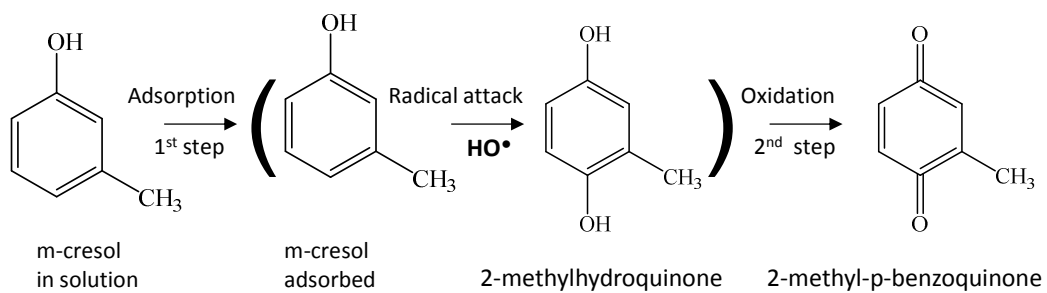
445 **Fig 7.** Continuous electro-Fenton with Fe-AC (28 mg Fe/L) treatment of MC at two
446 residence times (45 and 60 min); dotted lines correspond with the theoretic reduction
447 from the kinetic behaviour.

448

449

450 **Fig. 8.** Proposed reaction sequence on the degradation of MC by the heterogeneous
451 electro-Fenton with Fe-AC.

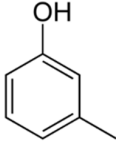
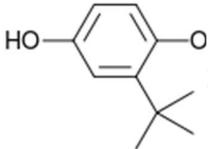
452



453

454

455 **Table 1.** Chemical formula and structure, CAS number and concentration of studied
456 compounds.

Compound	CAS number	Molecular formula	Structure	Concentration (mg/L)
m-cresol (MC)	108-39-4	C ₇ H ₈ O		100
Tert-butylhydroquinone (TBHQ)	1948-33-0	C ₁₀ H ₁₄ O ₂		100

457

458

459

460 **References**

- 461 1 V. Kavitha, K. Palanivelu *Water Res.*, 2005, **39**, 3062-3072.
- 462 2 C. Flox, P. Cabot, F. Centellas, J. A. Garrido, R. M. Rodríguez, C. Arias and E.
463 Brillas *Appl. Catal. B Environ.*, 2007, **75**, 17-28.
- 464 3 United State Environmental Protection Agency *M-Cresol and xyleneol*; EPA 738-F-
465 94-022: 1994.
- 466 4 CARB. California Air Resources Board, 2000.
- 467 5 Y. Ren, L. Peng, G. Zhao and C. Wei *Biochem. Eng. J.*, 2014, **88**, 108-114.
- 468 6 S. Dey, S. Mukherjee *J. Environ. Sci.*, 2013, **25**, 698-709.
- 469 7 L. Wang, Y. Yao, Z. Zhang, L. Sun, W. Lu, W. Chen and H. Chen *Chem. Eng. J.*,
470 2014, **251**, 348-354.
- 471 8 L. T. Markovska, V. D. Meshko and M. S. Marinkovski *J. Serb. Chem. Soc.*, 2006,
472 **71**, 957-967.
- 473 9 M. Choquette-Labbé, W. A. Shewa, J. A. Lalman and S. R. Shanmugam *Water*,
474 2014, **6**, 1785-1806.
- 475 10 S. Adishkumar, S. Kanmani *Desalin. Water Treat.*, 2010, **24**, 67-73.
- 476 11 Y. Zheng, D. O. Hill and C. H. Kuo *J. Hazard. Mater.*, 1993, **34**, 245-260.
- 477 12 C. Flox, C. Arias, E. Brillas, A. Savall and K. Groenen-Serrano *Chemosphere* , 2009,
478 **74**, 1340-1347.

- 479 13 M. Umar, H. A. Aziz and M. S. Yusoff *Waste Manage.*, 2010, **30**, 2113-2121.
- 480 14 E. Alfaya, O. Iglesias, M. Pazos and A. Sanromán *RSC Adv.*, 2015, **5**, 14416-14424.
- 481 15 O. Iglesias, J. Gómez, M. Pazos and M. A. Sanromán *Appl. Catal. B Environ.*, 2013,
482 **144**, 416-424.
- 483 16 A. Asghar, A. A. Abdul Raman and W. M. A. Wan Daud *J. Clean. Prod.*, 2014, **87**,
484 826-838.
- 485 17 X. Zhang, Y. Chen, N. Zhao, H. Liu and Y. Wei *RSC Adv.*, 2014, **4**, 21575-21583.
- 486 18 P. V. Nidheesh, R. Gandhimathi, S. Velmathi and N. S. Sanjini *RSC Adv.*, 2014, **4**,
487 5698-5708.
- 488 19 J. P. Guin, D. B. Naik, Y. K. Bhardwaj and L. Varshney *RSC Adv.*, 2014, **4**, 39941-
489 39947.
- 490 20 A. El-Ghenymy, R. M. Rodríguez, C. Arias, F. Centellas, J. A. Garrido, P. L. Cabot
491 and E. Brillas *J. Electroanal. Chem.*, 2013, **701**, 7-13.
- 492 21 N. Borràs, C. Arias, R. Oliver and E. Brillas *J. Electroanal. Chem.*, 2013, **689**, 158-
493 167.
- 494 22 Y. Wang, H. Zhao, S. Chai, Y. Wang, G. Zhao and D. Li *Chem. Eng. J.*, 2013, **223**,
495 524-535.
- 496 23 Y. Y. Chu, Y. Qian, W. J. Wang and X. L. Deng *J. Hazard. Mater.*, 2012, **199-200**,
497 179-185.

- 498 24 O. García, E. Isarain-Chávez, A. El-Ghenymy, E. Brillas and J. M. Peralta-
499 Hernández *J. Electroanal. Chem.*, 2014, **728**, 1-9.
- 500 25 A. El-Ghenymy, C. Arias, P. L. Cabot, F. Centellas, J. A. Garrido, R. M. Rodríguez
501 and E. Brillas *Chemosphere*, 2012, **87**, 1126-1133.
- 502 26 L. Feng, N. Oturan, E. D. van Hullebusch, G. Esposito and M. A. Oturan *Environ.*
503 *Sci. Pollut. Res.*, 2014, **21**, 8406-8416.
- 504 27 M. Panizza, E. Brillas and C. Comninellis *J. Environ. Eng. Manage.*, 2008, **18**, 139-
505 153.
- 506 28 B. P. Chaplin *Environ. Sci. Process. Impacts*, 2014, **16**, 1182-1203.
- 507 29 W. Liu, Z. Ai and L. Zhang *J. Hazard. Mater.*, 2012, **243**, 257-264.
- 508 30 O. Iglesias, E. Rosales, M. Pazos and M. A. Sanromán *Environ. Sci. Pollut. Res.*,
509 2013, **20**, 2252-2261.
- 510 31 K. Y. Foo, B. H. Hameed *J. Hazard. Mater.*, 2009, **171**, 54-60.
- 511 32 S. A. Messele, O. S. G. P. Soares, J. J. M. Órfão, C. Bengoa, F. Stüber, A. Fortuny,
512 A. Fabregat and J. Font *Catal. Today*, 2015, **240**, 73-79.
- 513 33 C. Chen, H. Chen, X. Guo, S. Guo and G. Yan *J. Ind. Eng. Chem.*, 2014, **20**, 2782-
514 2791.
- 515 34 D. De Beer, J. F. Harbertson, P. A. Kilmartin, V. Roginsky, T. Barsukova, D. O.
516 Adams and A. L. Waterhouse *Am. J. Enol. Vitic.*, 2004, **55**, 389-400.
- 517 35 R. M. Sellers *Analyst.* , 1980, **105**, 950-954.

- 518 36 K. Z. Elwakeel, G. O. El-Sayed and S. M. Abo El-Nassr *Desalin. Water Treat.*,
519 2014. DOI:10.1080/19443994.2014.919606.
- 520 37 M. M. Rahman, M. Adil, A. M. Yusof, Y. B. Kamaruzzaman and R. H. Ansary
521 *Mater.*, 2014, **7**, 3634-3650.
- 522 38 M. E. Ossman, M. Abdel Fatah and N. A. Taha *Desalin. Water Treat.*, 2014, **52**,
523 3159-3168.
- 524 39 A. Babuponnusami, K. Muthukumar *Chem. Eng. J.*, 2012, **183**, 1-9.
- 525 40 A. Rey, J. A. Zazo, J. A. Casas, A. Bahamonde and J. J. Rodriguez *Appl. Catal. A*
526 *Gen.*, 2011, **402**, 146-155.
- 527 41 M. S. Lucas, J. A. Peres *J. Hazard. Mater.*, 2009, **168**, 1253-1259.
- 528 42 Y. Chu, D. Zhang, L. Liu, Y. Qian and L. Li *J. Hazard. Mater.*, 2013, **252-253**, 306-
529 312.
- 530 43 V. K. Gupta, B. Gupta, A. Rastogi, S. Agarwal and A. Nayak *J. Hazard. Mater.*,
531 2011, **186**, 891-901.
- 532 44 V. K. Gupta, B. Gupta, A. Rastogi, S. Agarwal and A. Nayak *Water Res.*, 2011, **45**,
533 4047-4055.
- 534 45 G. Busca, S. Berardinelli, C. Resini and L. Arrighi *J. Hazard. Mater.*, 2008, **160**,
535 265-288.
- 536 46 E. Rosales, O. Iglesias, M. Pazos and M. A. Sanromán *J. Hazard. Mater.*, 2012, **213-**
537 **214**, 369-377.

- 538 47 E. Isarain-Chávez, C. De La Rosa, L. A. Godínez, E. Brillas and J. M. Peralta-
539 Hernández *J Electroanal Chem*, 2014, **713**, 62-69.
- 540 48 P. Liu, S. He, H. Wei, J. Wang and C. Sun *Ind. Eng. Chem. Res.*, 2015, **54**, 130-136.
- 541 49 Y. Ni, L. Wang and S. Kokot *Anal. Chim. Acta*, 2000, **412**, 185-193.
- 542 50 N. Izaoumen, N. B. Abderrazik, K. R. Tamsamani, S. Esplugas and E. Brillas
543 *Afinidad*, 2006, **63**, 449-453.
- 544